Research Article

Open Access

Synthesis, Characterization and Evaluation of Peanut Shells-Derived Activated Carbons for Removal of Methomyl from Aqueous Solutions

Magda A Akl[1*], Abdel Fatah M Youssef[1], Asaad H Hassan[2] and Heba Maher[1]

[1]Chemistry Department, Faculty of Science, Mansoura University, Mansoura, Egypt
[2]Chemistry Department, Faculty of Science, Damanhour University, Damanhour, Egypt

Abstract

Peanut shells-derived activated carbons (ACPNS) with different chemical characteristics, appropriate for the removal of methomyl pesticide in aqueous solutions are prepared. The steam activated carbon is obtained from the carbonized peanut shells in the presence of nitrogen in the temperature range from 973 to 1173K. The carbonized peanut shells are, further, chemically activated using NaOH and $ZnCl_2$. The structure of the ACPNS was characterized by N_2 adsorption at 77K, scan electron microscopy and FTIR. B.E.T methods are used to deduce the effective surface areas. The parameters (such as initial pH, temperature, etc) affecting the adsorption capacity of peanut shells-derived activated carbons toward methomyl removal from aqueous solutions are investigated using batch experiments. The study of kinetic models including pseudo first order and pseudo second-order are carried out. Adsorption isotherms are investigated. Equilibrium adsorption data fitted the Langmuir adsorption isotherm well with $R^2 > 0.9980$. The maximum adsorption capacities of peanut shells-derived activated carbons for the removal of methomyl, are calculated. The thermodynamic parameters including $\Delta G°$, $\Delta H°$ and $\Delta S°$ for the adsorption processes of methomyl on the ACPNS were calculated, and the negative value of $\Delta G°$ indicated the spontaneous nature of adsorption. The prepared peanut shells derived activated carbons are successfully applied to the removal of methomyl pesticide from different water samples with a recovery % > 95 and a RSD < 3%. The mechanism of adsorption is proposed.

Keywords: Methomyl; Pesticide; Peanut shells; Activated carbons; Adsorption

Introduction

Pollution of ground and surface water is considered as the most important problem can threaten human, animals, plants and aquatic organisms. One of the common reasons for water pollution is using pesticides which recently used in agriculture for killing insects, bacteria, fungus, and other things that feed on crops.

Pesticides are chemically and artificially synthesized compounds and it is considered as to be toxic bio accumulative agents [1]. There are several different types of pesticides such as herbicides, insecticides, nematocides and fungicides. Pesticides vary greatly in toxicity and they are potentially hazardous to living system and environment. Pesticides have harmful effects from dermal, oral and respiratory exposure. Such effects include carcinogenicity, liver damage, teratogenicity, oncogenicity, reproductive disorders, mutagenicity, nerve damage and allergenic sensitization [2]. So, pesticides have harmful effect and it constitute a threat for surface and ground water sources. This contamination occurs mainly through industrial wastewater discharges, leaching, surface run-off and deposition from aerial applications [3]. The maximum allowed concentration of total pesticides according to the European Union Directives and Regulations for drinking water hygiene is 0.1 µg/L [4]. Methomyl is one of different types of pesticides according to chemical structure. It is a highly toxic carbamate insecticide first registered in 1968 by the EPA as a "Restricted use pesticides" and is used on a wide variety of crops. It is a cholinesterase inhibitor and is often most effective against pests that have developed a resistance to organophosphates [5]. It dissolves rapidly in water and is not persistent in soil. The harmful effects of methomyl because its absorption through the skin or the lungs through oral exposure [6]. It is highly toxic when absorbed orally and moderately toxic when absorbed dermally and its chronic effects are similar to its acute effects [7,8]. Methomyl is highly toxic to fishes, aquatic invertebrates, birds and mammals [9]. It can be fatal to humans at relatively high doses. Because of its harmful effect and its toxic contamination there are different techniques for its removal from water supplies and for water purification. Some techniques include aerobic degradation [10], photo

catalytic degradation [10,11]. Ultrasound combined with photo-Fenton treatment [12], electro dialysis membranes [13], filtration, ozonation [14], reactions with oxidants such as free radicals, disinfection, floatation [15], preconcentration [16] and adsorption [17]. Amongst these techniques, adsorption is considered as the most effective and widely used for control of taste and odor as well as removing synthetic organic compounds and wide range of pollutants from wastewater and water supplies [18,19]. There are many advantages for using adsorption technique in water purification. It is low cost, easy, and simple system. There is no formation of byproducts after treatment by adsorption process and free from or less generation of toxic substances. Nowadays, there are many different adsorbents can be used for water treatment and purification such as silica gel [20], activated alumina [21], zeolites [22], polymers [23] & resins [24], clay [25] and activated carbon [26].

Peanut shells derived activated carbons are rarely used for the removal of organic pollutants from aqueous solutions [27,28].

To the best of our knowledge, no reported data is available regarding the use of peanut shells derived activated carbons in the removal of methomyl pesticide from aqueous solutions.

The objectives of the present study are the preparation, characterization and modification of peanut shells derived activated carbons (ACPNS). Peanut is an oil plant which is extensively cultured in Egypt. Peanut shells have low cost and are considered as waste matter in the environment. The peanut shells are modified physically by steam

*Corresponding author: Magda A Akl, Chemistry Department, Faculty of Science, Mansoura University, Mansoura, Egypt, Tel: 20502217833; E-mail: magdaakl@yahoo.com

and chemically using NaOH and ZnCl$_2$. The modified peanut shells derived activated carbons are thoroughly investigated for the removal of the methomyl pesticide from aqueous solutions. The different experimental factors affecting the removal of methomyl are studied viz. the influences of initial concentration of pesticide, contact time, dose of activated carbon and temperature on the adsorption capacities of peanut shell activated carbon for methomyl were investigated. In addition, kinetic and thermodynamic studies were established to expect the adsorption behavior.

Experimental

Reagents and solutions

Methomyl (Scheme 1) was purchased from Kafr El-Zayat Pesticides & Chemicals Company, Kafr El Zayat, Gharbia, Egypt. A stock solution of 1000 ppm of methomyl was prepared by dissolving 1 g in 1 L distilled water. Peanut shells were obtained from local markets in Egypt. NaOH, ZnCl$_2$ and HCl were purchased from Sigma-Aldrich.

Apparatus

The pH measurements were made using a pH meter (Hi 931401, HANNA, Portugal). The concentration of methomyl was analyzed using UV-Vis spectrophotometer (Chrom Tech-Co., Ltd., USA). The adsorbents were weighed using analytical balance. Water bath shaker was used for adsorption experiments.

Peanut shells were crushed, washed with 0.5% HCl to remove all dirt, dried in an oven at 378K for overnight, ground by a mill, sieved to mesh size of 1-4 mm and carbonized in a tabular furnace at 873K for 2 h.

Carbonized material was soaked in sodium hydroxide (NaOH) solution with two impregnation ratios of char: NaOH (w/w) equal to 1:1 (CN11) and 1:3 (CN13) for 24 h. The two mixtures were then dehydrated in an oven overnight at 378K to remove moisture and then activated at 1023K for 2 h. The resulting AC was washed with distilled water several times after cooling until pH of filtrate reached to (7-8). This was followed by drying of the AC overnight in an oven at 378K.

Zinc chloride activated carbon samples were prepared by soaking dried peanut shells in zinc chloride with two impregnation ratios viz. carbonized peanut shell: ZnCl$_2$ (w/w) equal to 2:1 (CZ21) and 1:2 (CZ12). The two mixtures were dried in an oven at 378K overnight to remove moisture and then activated at 873K for 2 h. Then, the AC was washed with distilled water several times till filtrate from chloride ions. This followed by drying the two samples in an oven at 378K overnight.

Activation of carbonized peanut shells with steam flow equal to 150 ml/min with different times to obtain 20% and 48% burn-off of activated carbon samples (CS20 and CS48).

Characterization of adsorbents

The BET surface area (S$_{BET}$) measurements of the carbons were made by nitrogen adsorption at 77K using surface Area& Size Analyzer (QUANTACHROME- NOVA 2000 Series). The surface micrographs of the carbons were taken by using a scanning electron microscope JSE - T20 (JEOL, Japan). The instrument was operated at 40 kW. Prior to the analysis, the samples were dried at 383K for 4 h. A thin layer of gold was coated on the samples for sample metallization and charges dissipation.

Fourier transform infrared spectroscopy (FT-IR) technique was used for qualitative measurements of functional groups present on the activated carbon surface. By using Jusco instrument (Model 6100, Japan), Sample discs were prepared by mixing 1 mg of the samples with 500 mg of KBr (Merck) in an agate mortar and scanned in a range from 4000 to 400 cm^{-1}.

Surface acidity and Boehm titration technique was applied for determination the type and amount of functional groups on the carbon surfaces by neutralization with bases of various strengths.

Adsorption experiments

Batch sorption experiments were done by shaking 0.02 g of activated carbon with 50 ml aqueous solution of methomyl in 250 ml-Erlenmeyer flasks placed in a temperature controlled shaking water bath at different concentrations (between 100 and 1600 mg/l), pHs (between 2 and 12), ionic strength (between 0.002 and 0.09 mole/l), temperatures (between 289 and 313K) and sorbent doses (between 0.01 and 0.02 g) at a constant shaking rate of 125 rpm. The amounts of pesticide removed by sorbents (qe) Eqn (1) and percent removed (R %) Eqn (2):

$$q_e = \frac{(C_o - C_e)}{m} \times 100 \tag{1}$$

$$\%R = \frac{(C_o - C_e)}{C_o} \times 100 \tag{2}$$

Where q_e is the amount of pesticide adsorbed (mg/g). C_o and C_e are the initial and equilibrium liquid-phase concentrations of pesticide (mg/g), respectively. V is the volume of the solution (L), and m is the weight of the sorbent used (g).

Results and Discussion

Characterization of the adsorbents

Textural properties

The nitrogen adsorption-desorption analysis: The surface area and porosity of carbons are prominent factors in determining their adsorption capacities [29,30]. The textural properties of solids are conventionally determined from the adsorption of nitrogen at 77K and the adsorption data are usually analyzed by the application of the BET equation [31,32].
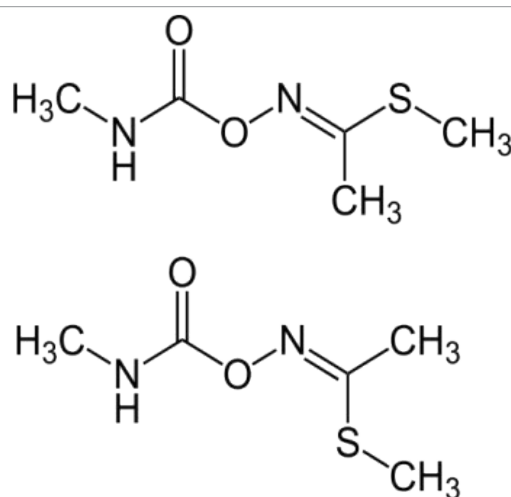
Scheme 1: Chemical structure of methomyl.

The adsorption of nitrogen by the carbons investigated was found to be relatively rapid with the equilibrium attained within 25 min indicating that the adsorption is not controlled by activated diffusion encountered in ultrafine pores and meanwhile refers to the accessibility of the entire pore structure to the nitrogen molecules [33]. Figure 1 depicts the nitrogen adsorption isotherms measured at 77K for the carbons C, CS20, CS48, CZ21, CZ12, CN11 and CN13.

For carbon C, the isotherms is mainly type I according to the BDDT classification with no hysteresis loop [34]. The isotherms of ACPNS show mixed characteristics of type I and type IV; they are less steep and exhibited closed hysteresis loops.

The values of surface area of the ACPNS samples were calculated from the linear BET plots of N_2 adsorption at 77K. The results are represented in Table 1 depicts:

(i) The surface area for non-activated carbon is very low compared to activated carbon due to the absorption of activating agent NaOH, $ZnCl_2$ or steam. The S_{BET} of CN13 is 35.5 times more than C, while CS48 is 20.8 times more than C and CZ12 is 26.8 times more than C.

(ii) The NaOH activated carbon (CN13) sample possesses higher surface area value than other ACPNS.

(iii) The S_{BET} values of CN13 increased from 1242.86 m²/g to 2362.85 m²/g when the char: NaOH ratio increased from (1:1) to (1:3) because of increasing the impregnation ratio.

(iv) Increasing the impregnation ratio of $ZnCl_2$ led to an increase in SBET values from 1449.03 m²/g to 1783.52 m²/g with increasing of precursor: $ZnCl_2$ from (1:2) to (2:1) ratio which is designed as CZ12 and CZ21 samples, respectively.

(v) The S_{BET} of steam activated carbon increased from 801. 55 m²/g to 1388.00 m²/g, with increasing the burn off degree for CS20 and CS48 samples, respectively.

(vi) The Total pore volume of non-activated sample is very low compared to activated ones and (ml/L) increased with activation and with increasing of % of activating agents.

(vii) The pore radius ranged between 0.389 and 0.514 nm for the activated samples.

Scanning electron microscopy (SEM): The scanning electron microscopy images gave insight into the peanut shells structure with respect to its shape. The dark areas are macro pores and the pale grey
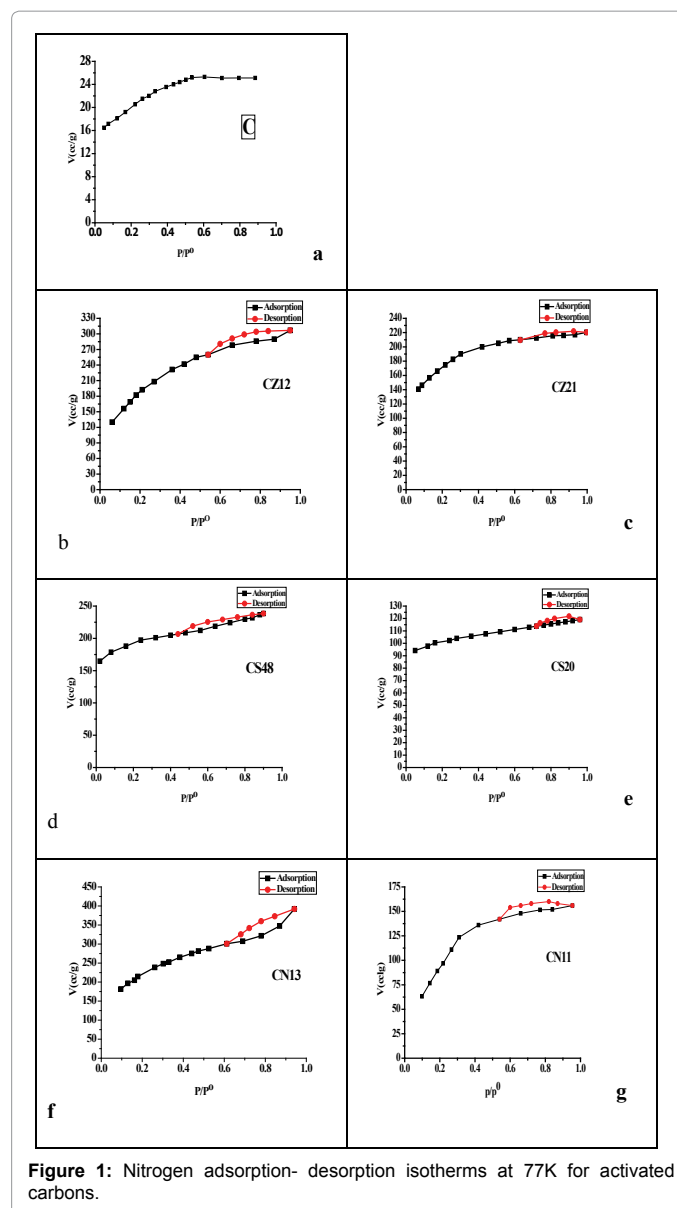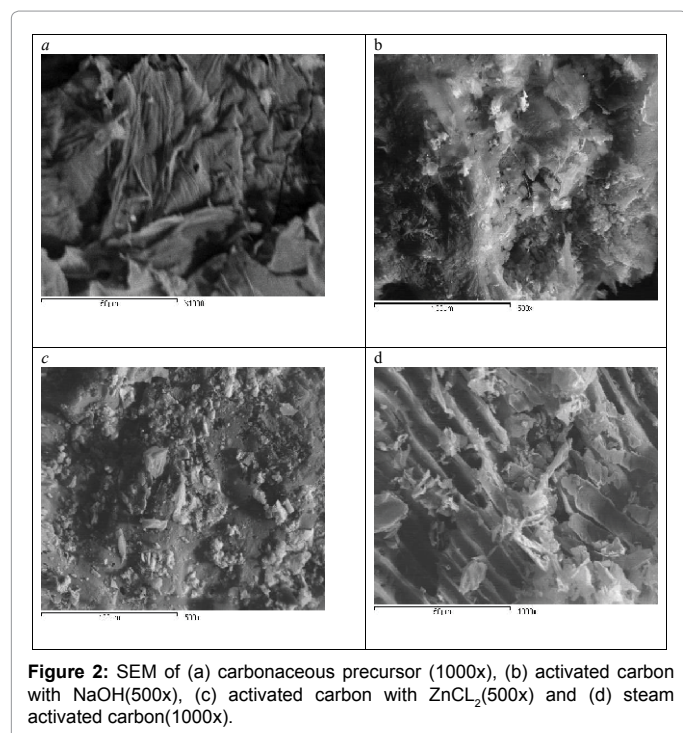

Figure 1: Nitrogen adsorption- desorption isotherms at 77K for activated carbons.

areas are due to the carbon matrix. Figure 2 represents the morphology of the resulting activated carbon prepared via physical (CS) and chemical (CN11, CN13, CZ12, CZ21) activation methods, respectively. It can be clearly seen that physical and chemical activations show some changes in the surface of the particles after activation. The different pore structures of the activated carbon prepared from either physical (using steam as activating agent) or chemical (using NaOH or $ZnCl_2$) activation are observed, which depend upon different reaction mechanisms. Figure 2 depicts four pictures (a) carbonaceous precursor, (b) for chemically activated carbon using NaOH, (c) chemically activated using $ZnCl_2$ and (d) physically activated carbon (CS). In this concern, the sample (d) activated by steam indicated that the carbon matrix are greater than the dark areas. This is referred to the nature of the micropores resulting from the activating steam. The dark areas are greater than the carbon matrix using NaOH or $ZnCl_2$ as activators in chemical activation. This implies to the higher surface area of samples (b, c) due to mesopores as well as to micro-pores.

Sample	SBET(m²/g)	VT(ml/g)	r (nm)
C	66.640	0.039	1.167
CS20	801.550	0.189	1.272
CS48	1449.002	0.342	1.493
CZ21	1270.030	0.336	1.464
CZ12	1783.520	0.476	1.533
CN11	1242.860	0.242	1.389
CN13	2362.850	0.608	1.655

Table 1: N_2 adsorption and surface area data.

Figure 2: SEM of (a) carbonaceous precursor (1000x), (b) activated carbon with NaOH(500x), (c) activated carbon with ZnCL$_2$(500x) and (d) steam activated carbon(1000x).

Also, this shows that the peanut shells activated by NaOH and ZnCl$_2$ have irregular carbon matrix. i.e., of different shapes and sizes. This was proved by nitrogen adsorption isotherms of activated peanut shells which indicated that they were mainly micro pores only in physical activation and a mixture from micro- and mesopores in chemical activation. This may be explained by progressive changes in the surface of the cellular structure of the parent material with NaOH and ZnCl$_2$ solution used as shown in Figure 2. The cellulose units are hydrolyzed or dehydrated by the chemicals used and thus the main components of the intercellular wall are broken down to smaller structure. Thus it is apparent that the external surface of peanut shells is quite rough, consisting of cavities, cracks, and irregular protrusions.

Chemical properties: The chemistry of the surface of a carbon is more important than its textural properties in determining its adsorption capacity of pests from aqueous solution particularly when the adsorption involves interaction with the surface functional groups via ion exchange and/or complex formation which is most probably the case in adsorption of pests on activated carbons.

FTIR: The chemistry of the carbon surface is attributed to the existence on the surface of carbon-oxygen functional groups of acid or basic character. The FTIR spectra of samples ACPNS (before and after adsorption of methomyl) have been recorded, Figure 3. The recorded IR spectra of CZ21, CN11 and CS20 (before adsorption of methomyl) depicts: the existence of a broad band around (3414-3446) cm^{-1} that is attributed to O-H stretching vibrations due to the presence of free hydroxyl groups, bonded O-H bands of carboxylic acids and adsorbed water [35,36]. The peaks observed around (1034-1116) cm^{-1} are attributed to the C-O group in carboxylic and alcoholic groups [35-38]. The peaks observed around (610-875) cm^{-1} are attributed to in and out plane ring deformation in benzene derivatives [35,38,39].

The FTIR spectra of ACPNS after adsorption of methomyl show the following changes:

In CZ21-M : The appearance of a peak at 1630 cm^{-1} due to N-H bend denoting the presence of primary amines [40] and appearance of the peak at 1101 cm^{-1} due to C-O stretching due to presence of alcohols, carboxylic acids , esters and ethers [37].

For CN11-M: The disappearance of the peaks at 2116 cm^{-1} and peaks at 1391 cm^{-1}. This indicates the absence of –C≡C– stretch of alkyne groups and absence of C-C stretch (in- ring) of aromatic rings, respectively.

Finally, CS$_{20}$-M graph shows disappearance of peaks at 2103 cm^{-1}, 1430 cm^{-1} and 1057 cm^{-1} indicating the absence of –C≡C– stretch of alkyne groups , absence of C-C stretch (in- ring) of aromatic rings and C-H stretch of aliphatic amines, respectively. Also, new peak appeared at 1100 cm^{-1} due to C-O stretch which indicates the presence of alcohols, carboxylic acids, esters or amines groups [41].

Surface acidity and Boehm titration: The pH of the aqueous slurry of the carbon material provides a convenient indicator of the type and concentration of the chemical parameters of the ACs investigated. Table 2 reveals that (i) the surface pH of carbon C is (7.9) indicating its surface basicity, i.e the basic functional groups on the surface of non-oxidized carbon are more dominating compared with those of the acid type. The same is also true for steam activated ACPNS of surface pH= 8.2 and 8.3. Steam activation at 1223K usually leads to the formation on the carbon surface of C-O groups of basic character [42]. Treatment with NaOH (CN11, CN12) increased the surface pH from 7.98 to 8.77 and 8.90 for CN11 and CN12, respectively. On the other hand, treatment with ZnCl$_2$ increased the total acidity increase from 7.98 to 6.66.
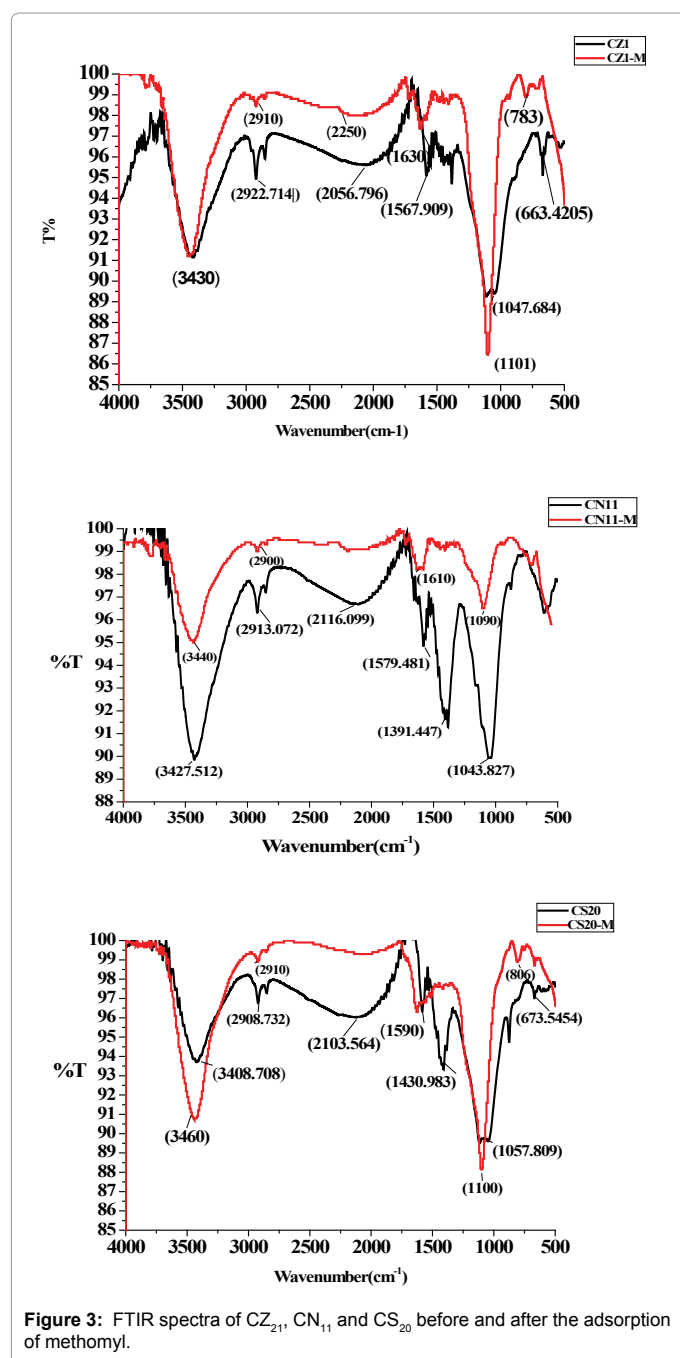
The pH of zero point charge pH pzc of ACPNS ranged between 7.0 and 8.8 for activated samples due to the effect of basic function groups.

The surface acidic groups could be determined in (m.eq/g) by the selective neutralization with a series of bases of varying strength, viz. NaHCO$_3$, Na$_2$CO$_3$, NaOH and NaOC$_2$H$_5$. NaHCO$_3$ neutralizes carboxylic groups where as those neutralized by Na$_2$CO$_3$ but not by NaHCO$_3$ are lactones. The weak acid groups neutralized by NaOH but not by Na$_2$CO$_3$ were postulated as phenols. The groups reacting with NaOC$_2$H$_5$, but not with NaOH, were suggested to be carbonyl groups [43]. Table 2 shows the surface acidity and the abundance of different acidic groups on the surface of non-activated and activated carbon samples.

The ash content in case of NaOH and steam activated carbon is high due to loss of carbon content by H$_2$O (steam) or NaOH as activating agent and it is low in case of ZnCl$_2$ sample due to volatilization effect of ZnCl$_2$ on ash content.

Adsorption of methomyl

Effect of pH: The pH value of the solution, which affects the surface charge of the adsorbent and the degree of speciation of adsorbate was an important controlling parameter in the adsorption process. The chemical name of methomyl is S-methyl N-(methylcarbamoyloxy) thioacetimidate and the molecular weight is 162. According to the physicochemical properties of methomyl reported in Hazardous Substances Data Bank [29], the hydrolysis half-life of methomyl in aqueous environment depends on the pH value of the solution. Therefore, the effect of pH value of the solution on methomyl was investigated with the results presented in Figure 4. The results obtained revealed that, in the pH range of 2 to 8, the methomyl is rather stable. In contrast, when the pH value rises to 10, the residual amount of

Figure 3: FTIR spectra of CZ_{21}, CN_{11} and CS_{20} before and after the adsorption of methomyl.

due to the presence of excess H^+ ions competing with positively charged methomyl molecules for the sorption sites of sorbents. Furthermore, at lower pH values (below the pKa of carboxylic groups, approximate 4.6), the -COO- groups in ACPNS are protonated to -COOH groups and the hydrogen bonds between -COOH and $-NH_2$ groups are formed resulting in a decrease of methomyl uptake. Also, the repulsion between positively charged amino group of ACPNS and cationic pesticide molecules resulted in decrease pest removal in acidic medium.

Effect of initial methomyl concentration: The effect of initial concentration on the removal of methomyl by ACPNS was studied at different temperatures at normal pesticide pH. The results are graphed in Figure 5. It is seen that the equilibrium sorption capacities of the sorbents increase with an increase in initial pest concentration and the adsorption at different concentrations is rapid in the initial stages and gradually decreases with the progress of adsorption until the equilibrium is reached. This may be attributed to the fact that, the higher the initial methomyl concentration, the greater the driving force of the concentration gradient at solid-liquid interface which cause an increase of the amount of methomyl adsorbed on the adsorbent. At higher methomyl concentration adsorption capacity reached a plateau indicating saturation of the available binding sites on the adsorbents. The steep slope at initial methomyl concentrations is a desirable feature of the sorption system and the results indicates that the ACPNS are efficient adsorbents for methomyl.

Effect of adsorbent dosage: An experiment was made to study the effect of adsorbent dosage on methomyl adsorption. Various quantities of CN13 as selected ACPNS sample were added to a fixed initial pesticide concentration. The uptake of methomyl after a contact time of 24 h versus the adsorbent dosage (g/L) used is shown in Figure 6. It can be noticed that the methomyl uptake increased from 19 to 87% when CN13 dose was increased from 0.12 to 1.57 g/L, respectively. This is due to the fact that as the adsorbent dosage is increased, more adsorption sites are available for adsorbate enhancing the methomyl uptake [44]. Also, with increasing adsorbent loading, the quantity of methomyl adsorbed on to the unit weight of the adsorbent is reduced causing a decrease in q_e (mg/g) values with increasing activated carbon loading.

Effect of contact time: Figure 7 shows the effect of contact time on the adsorption capacity of CN13, as an example, for methomyl. The adsorption capacity of CN13 increased rapidly with the increase of contact time from 0 to 20 min and more than 90% of the equilibrium adsorption capacity for methomyl occurred within 15 min. After 60 min, the adsorption capacity became constant and the adsorption reached equilibrium. Therefore, 60 min was selected as the contact time for the adsorption of methomyl onto the ACPNS under our experimental conditions.

As shown, the adsorption process was divided into three stages: (1) an initial stage with adsorption occurring instantly, (2) subsequently, slow adsorption, and (3) a final stage with adsorption reaching equilibrium and remaining constant. The first stage can be attributed to the rapid attachment of methomyl to the surface of the ACPNS by surface mass transfer. At this stage, more than 80% of methomyl adsorption was found in all cases. The second stage was slower, possibly because many of the available external sites was already occupied and because of the slow diffusion of methomyl molecules into the network of the ACPNS. An asymptotic trend was found after approximately 20 min regardless of the initial methomyl concentration applied to the adsorption system. The amount adsorbed did not vary significantly at contact times longer than the equilibrium time (60 min). The kinetics of the adsorption process indicates that the adsorption of methomyl

methomyl is only 12% of the original. Moreover, at high pH value of 12, methomyl is completely degraded to other compounds, interpreting that methomyl is degraded quite substantially in the basic solutions. Therefore, the effect of pH value on adsorption capacity was examined in the pH range of 2-8. As illustrated in Figure 4, the adsorption capacity decreases with increasing pH value, indicating that the lower pH value of solution enhances the adsorption of methomyl. ACPNS are weak base anions with pHpzc (point of zero charge) 7-8 as shown in Table 3. The adsorption of methomyl on ACPNS may be mainly due to dispersion forces and polarization of π electrons (electron-rich portion of the adsorbate).

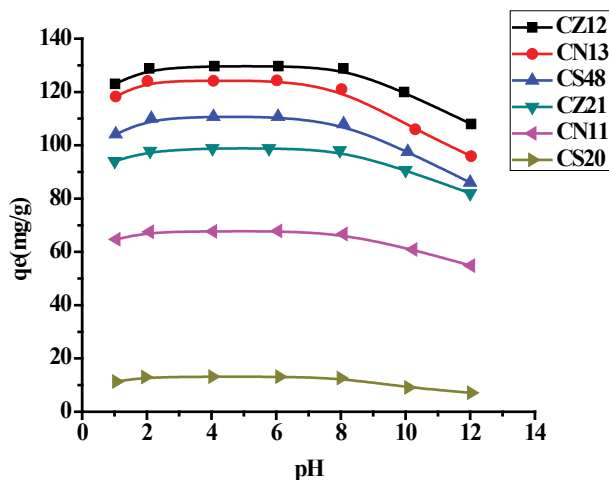On contrary, the lower pest removal at acidic pH(<2) is probably

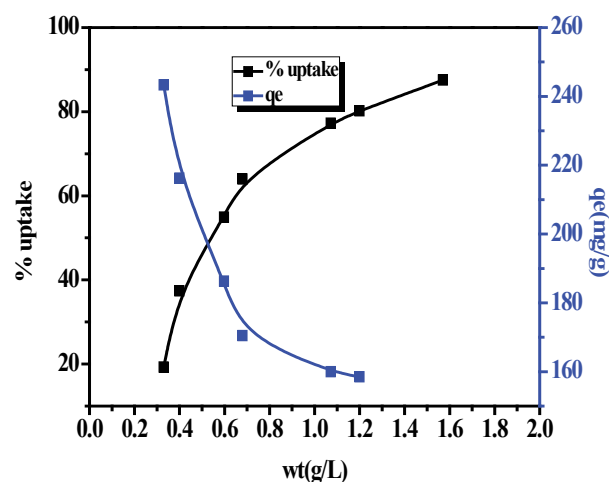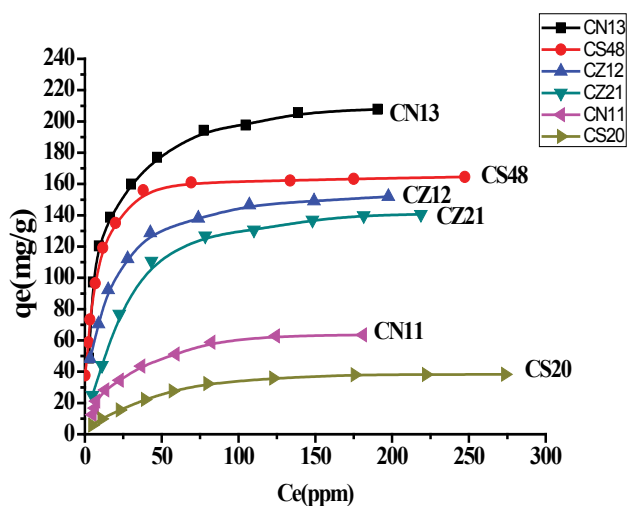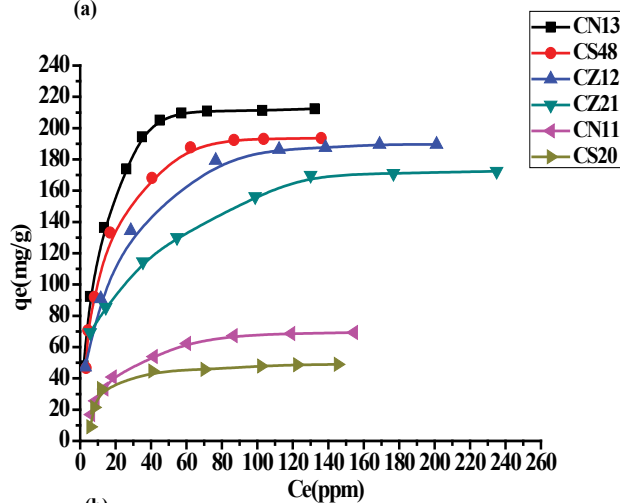**Figure 4:** Effect of pH on the adsorption capacity of methomyl on different ACPNS carbons.

Figure 6: Effect of mass on the adsorption of methomyl on NaOH activated carbon CN13 sample.

Figure 5: Effect of initial methomyl concentration on the adorption capacity of ACPNS (a) at 289 and (b) at 313K.
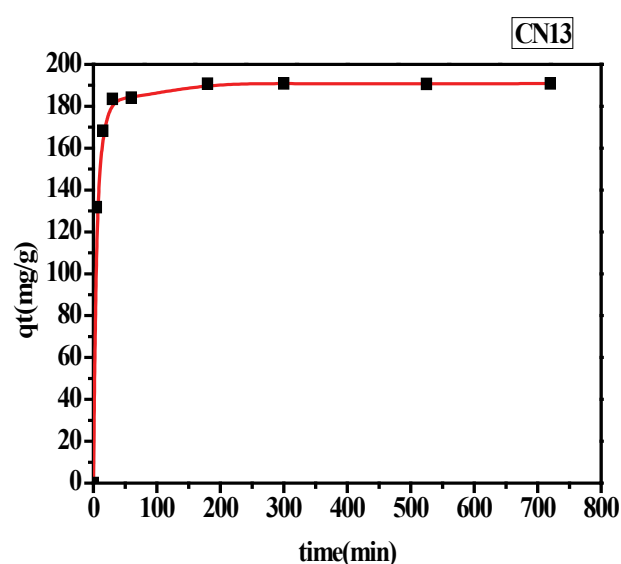

Figure 7: Effect of time on the adsorption of methomyl on NaOH activated carbon CN13 sample.

onto ACPNS can be considered as a fast adsorption process because more than 80% of methomyl was adsorbed within 20 min especially at methomyl concentration lower than the maximum adsorbed. Such findings reveal the benefits of using this low-cost adsorbent or so-called eco-adsorbent for the treatment of aqueous solutions rich in pesticides in general and methomyl in particular.

Effect of ionic strength: The removal of pesticides from aqueous solutions depends greatly on electrostatic parameters such as surface charge, pH and ionic strength [45]. Ionic strength plays a major role in the electrical double layer (EDL) structure of a hydrated particle. The thickness of the DEL decreases as the ionic strength increasing, resulting in a decrease in adsorption [46]. In this work, the effect of the additional amounts of NaCl over a concentration range 0.002-0.05M was studied at the natural pH of methomyl (6.0). The results obtained revealed that that the adsorption capacities decreased with increasing NaCl concentration for the adsorbent. The ionic strength increases

as NaCl concentration increases and more Na^+ ions can screen the negative sites of the adsorbent, leading to the reduce of electrostatic attractive force, and accordingly, the amount adsorbed of methomyl decreases. The ionic strength may also lead to the dimerisation process of methomyl molecules, thereby reducing electrostatic force in the presence of high concentration of Na^+ and Cl^- ions.

Further increase in ionic strength above 0.05M decrease the adsorption capacities sharply until 0.15M where any further increase caused steep decrease in adsorption capacities because of salting out of pesticide molecules from aqueous solution. These results showed that ionic strength had an adverse effect on the pesticide adsorption, which may be induced by the competition between the cations and the pesticide for the electron rich sites.

Effect of temperature: The adsorption of methomyl on ACPNS was studied at different temperatures, and the results are shown in Table 3. The amount of methomyl adsorbed increased with a rise in temperature which means that methomyl adsorption from aqueous solutions on both modified and unmodified carbons is an endothermic process. The enhancement of adsorption capacity may be due to a chemical interaction between adsorbate and adsorbent, creation of some new adsorption sites, or an increased rate of intra particle diffusion into the pores of the adsorbant at higher temperature [38,39]. When the temperature increased from 289K to 313K, the maximum amounts of methomyl removed by ACPNS.

Adsorption isotherms

In equilibrium analysis, Langmuir [3] and Freundlich [4] models are the most frequently employed isotherm models for studying frequently employed isotherm models for studying the behavior and system of adsorption. Langmuir and Freundlich isotherms for the studied system at different temperatures are presented in Figures 8 and 9, respectively.

Table 3 shows also Langmuir's and Freundlich adsorption parameters for different adsorption at 289 and 313K. Inspection of Table 3 depicts: (i) Adsorption of methomyl onto ACPNS adsorbents follow both of Freundlich and Langmuir models as proved by correlation coefficient (R^2) which ranged between 0.996 and 0.999. The best fit model for adsorption of methomyl on all samples is Langmuir

adsorption model. (ii) As temperature increased, the adsorption capacities increased which indicates an endothermic nature for the all process of methomyl adsorption;(iii) As the ratio of activating agent increased as in $ZnCl_2$ or NaOH there was an increase in the adsorption capacities of the activated samples.

$$\frac{c_e}{q_e} = \frac{1}{bq_m} + \frac{c_e}{q_m} \tag{3}$$

$$\log q_e = \log K_F + \frac{1}{n}\log C_e \tag{4}$$

Adsorption kinetics

In order to understand the process of adsorption, four kinetic models were applied to analyze the experimental data. The linear form of pseudo first-order kinetic model of Lagergren [47], rthe linear form of Ho's pseudo second-order kinetics [48], Intra-particle diffusion model [49] and Boyd model [5]. In this study, the four models were tested for methomyl on ACPNS. The best-fit model was determined depending on the linear correlation coefficient R^2. The results are shown in Figure 10 a,b and represented in Table 4.

$$F(t) = 1 - \frac{6}{\pi^2}\sum_{n=1}^{\infty}\frac{1}{n^2}\exp(-n^2 Bt) \tag{5}$$

The correlation coefficient of pseudo second-order which was close to unit was much higher than that of pseudo first-order and the theoretical q_2e value computed from pseudo second-order was much closed to the experimental q_{exp} value given in Table 4, indicating that the pseudo second-order model was more applicable for the system, while theoretical q_1e value estimated from pseudo first-order kinetic did not give reasonable value, suggesting this model could not be used to depict the adsorption data of methomyl onto the adsorbent.

For determination of the adsorption mechanism and prediction of the rate limiting step in adsorption process to understand the phenomena of adsorption the intraparticle diffusion and Boyd models were applied. For intraparticle diffusion, Figure 10c, the results obtained indicated that the plot of q_t against $t^{0.5}$ of CN11 for

Sample	Boehm	titration	pHPCZ		pH of supernatant	Loss on content	Ash
	Carboxylic (meq/g)	Phenolic (meq/g)	Lactonic (meq/g)			drying %	%
P	0.018	0.042	0.638	6.00	5.10	5.60	1.22
C	0.020	0.002	0.474	8.00	7.98	4.01	2.57
CH	0.482	0.096	0.916	3.00	2.18	2.31	0.42
CS20	0.010	0.115	0.147	8.00	8.20	3.71	4.16
CS48	0.001	0.112	0.089	8.20	8.30	3.44	7.62
CZ12	0.034	0.012	0.418	7.00	6.57	3.95	0.90
CZ21	0.074	0.014	0.288	7.20	6.66	5.48	1.00
CN11	0.000	0.081	0.115	8.60	8.77	2.71	8.88
CN13	0.000	0.010	0.034	8.80	8.90	4.18	17.93

Table 2: Characterization of activated carbon samples.

Sample	T=289K						T=313K					
	Langmuir constants			Freundlich constants			Langmuir constants			Freundlich constants		
	Qe (mg/g)	b(L/mg)	R²	K	n	R²	Qe(mg/g)	b(L/mg)	R²	K	n	R²
CS20	41.67	0.040	0.997	1.79	1.50	0.997	50.00	0.150	0.999	32.43.	12.20	0.996
CS48	166.67	0.250	0.999	51.94	3.15	0.993	212.77	0.100	0.999	39.92	2.58	0.997
CZ21	142.86	0.023	0.999	28.96	2.47	0.995	200.00	0.037	0.998	29.22	2.18	0.999
CZ12	166.67	0.083	0.999	75.19	8.47	0.999	204.08	0.089	0.998	40.85	3.50	0.996
CN11	71.43	0.049	0.999	8.36	2.24	0.993	80.00	0.057	0.998	10.49	2.34	0.997
CN13	217.39	0.092	0.999	65.24	3.86	0.992	250.00	0.138	0.998	48.38	2.58	0.997

Table 3: Langmuir and Freundlich isotherms constants for adsorption of methomyl on activated carbons.

methomyl is multilinear containing at least three linear segments which indicates that three steps occur during adsorption process. The first sharper portion is transport of pest molecules from the bulk solution to the adsorbent external surface by diffusion through the boundary layer (film diffusion). The second portion is the diffusion of the pest molecules from the external surface into the pores of the adsorbent. The third portion is the final equilibrium stage, where the pest molecules were adsorbed on the active sites on the internal surface of the pores and the intra-particle diffusion starts to slow down due to the solute concentration getting lower and lower in solution [50,51]. Also, the linear portion of the curve did not pass through the origin, suggesting that pore diffusion is not the step controlling the overall rate of mass transfer at beginning of adsorption. In Table 4, the correlation coefficients (R^2) for the linear segment intra-particle diffusion model was 0.307 indicating that the intra-particle diffusion was not the only rate controlling step; other process could control the rate of adsorption.

So, Boyd kinetic model (Figure 10d) was applied to predict the slow step involved in the adsorption process. For Boyd kinetic model, the results obtained indicated that the linear plot of $B(t)$ against (t)of CN11 for methomyl doesn't pass through the origin indicating that the adsorption process is controlled by film diffusion.

Thermodynamic studies

To determine the effect of temperature on methomyl adsorption, adsorption experiments were also conducted at 16 and 40°C, respectively. As shown in Figure 5, the adsorption capacity of methomyl onto ACPNS clearly increases with rising temperature, indicating an endothermic reaction. The thermodynamic parameters such as the change in Gibbs free energy (ΔG^o, kJ/mol), enthalpy (ΔH^o, kJ/mol) and entropy (ΔS^o, J/(mol•K)) are calculated [52].

The thermodynamic parameters for methomyl adsorption onto ACPNS are shown in Table 5. The positive value of $\Delta H°$ reflects an endothermic nature of methomyl adsorption ACPNS and indicates that the adsorption is favored at high temperature, which is supported by the increase of methomyl adsorption onto ACPNS with rising temperature. The adsorption is more favorable at higher temperature and methomyl was strongly adsorbed on the surface of both ACPNS.

The negative $\Delta G°$ indicates that the adsorption process is spontaneous. The magnitude of ΔG^o increased with increasing temperature, which also indicated that better adsorption was actually obtained at higher temperatures, because a more negative $\Delta G°$ implied a greater driving force of adsorption, resulting in a higher adsorption capacity.

The positive $\Delta S°$ suggests increased randomness at the solid/solution interface during lead adsorption [53,54].

Mechanism of adsorption

Modification of the carbon surface via steam, NaOH or $ZnCl_2$ introduces a variety of carbon oxygen functional groups of acidic nature. These groups dissociate in aqueous solutions and participate in the metal binding process. It is likely that other surface oxygen atoms (some of them may not be a component of protonogenic functional groups) may participate in complex formation. Thus, one would expect an ion exchange between methomyl with the H^+ released from the carboxylic and phenolic surface groups and therefore these groups contribute significantly to the enhancement of pesticide uptake. Carbonyl and/or lactonic groups, on the other hand are more likely involved in a complex formation with methomyl [55].

Analytical application

The prepared ACPNS were successfully applied for the removal of known amounts of methomyl spiked to different natural water samples. The recovery % ranged between and with a relative standard deviation (RSD, %, <3).

Conclusion

The results of the present study reveal that ACPNS may be extremely viable adsorbent for application in the removal of methomyl from aqueous solutions. Modification of ACPNS by steam, NaOH and $ZnCl_2$ significantly increased the oxygen-containing groups on the surface of activated carbons with noticeable change in the surface morphology and textural properties. The adsorption of methomyl was dependent on initial concentration, reaction temperature and pH. The methomyl adsorption capacity increased with the increase of pH in the range of 3-8, where ionization of carboxylic group occurs.

First –order kinetic equation			Second-order kinetic equation			Intraparticle diffusion equation			Boyd equation		qe,exp(mg/g)
q_1(mg/g)	K_1(1/min)*10^3	R^2	q_2(mg/g)	K_2(g/mgmin)*10^4	R2	K_{int}(mg/(g min$^{1/2}$))	C	R^2_{int}	I	R^2	
31.77	-3.365	0.377	192.31	2.97	0.999	1.59	159.66	0.307	0.249	0.849	217.39

Table 4: Kinetic parameters for adsorption of methomyl on CN11.

Sample	-ΔG°(KJ/mol)		ΔH°(KJ/mol)	+ΔS°(J/mol.K)
	289K	313K		
CS20	14.43	18.22	41.43	190.00
CS48	20.00	21.68	28.72	70.02
CZ21	17.76	18.67	14.90	113.00
CZ12	19.25	20.19	2.19	75.00
CN11	16.25	18.06	4.74	73.00
CN13	19.78	21.36	12.71	109.10

Table 5: Thermodynamic coefficients for methomyl adsorption onto activated carbons.

Figure 8: Langmuir plots (a) at 289K, (b) at 313K.

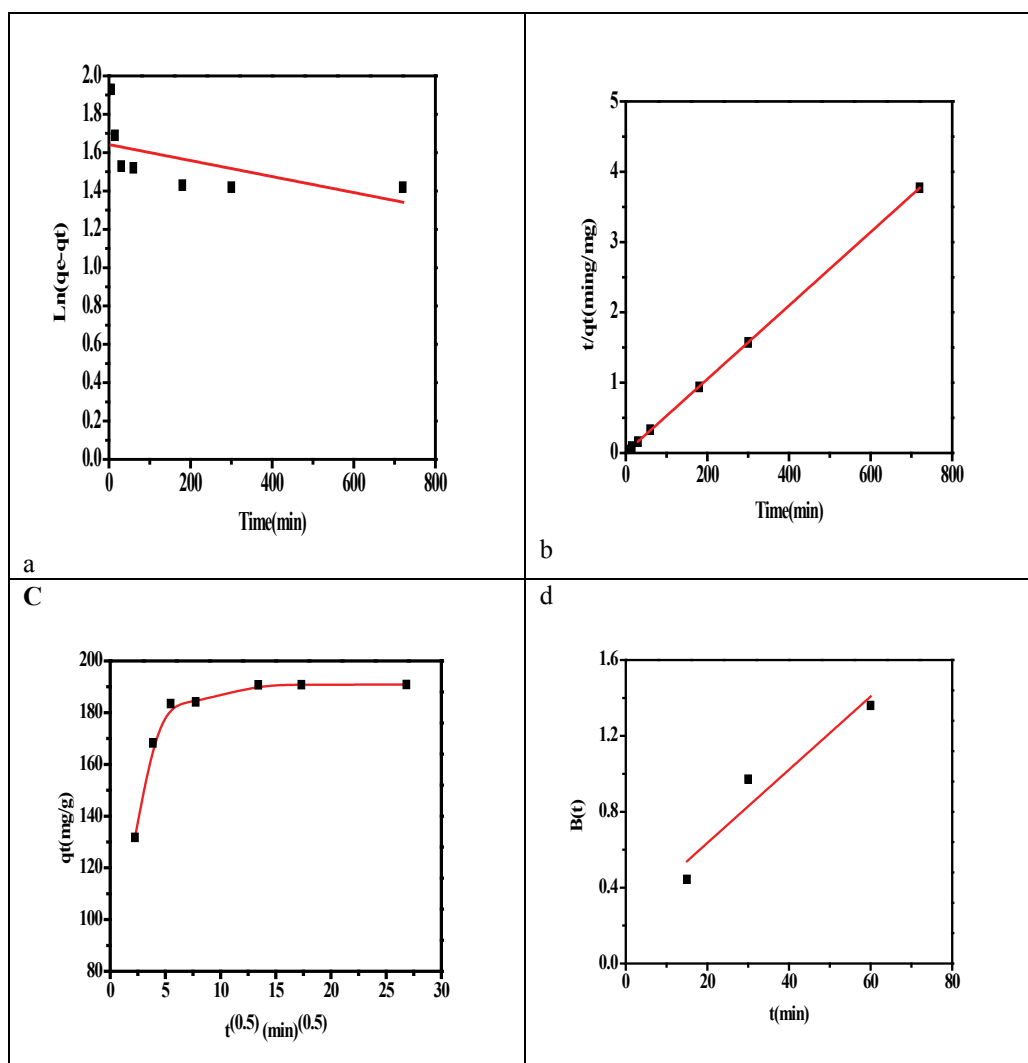**Figure 9:** Freundlich plots at (a) 289K, (b) 313K.
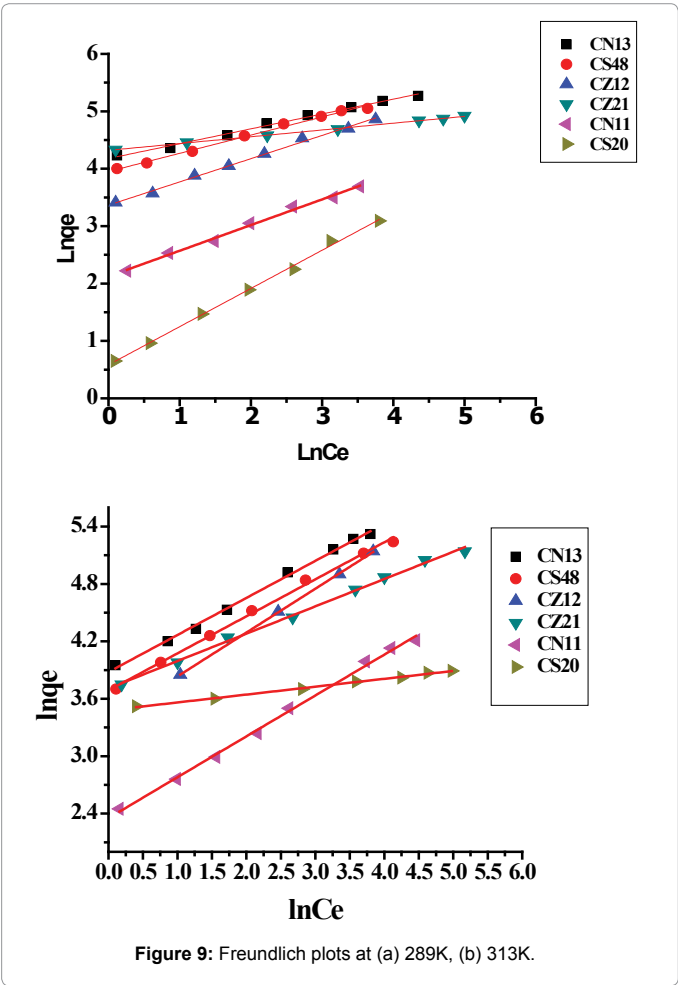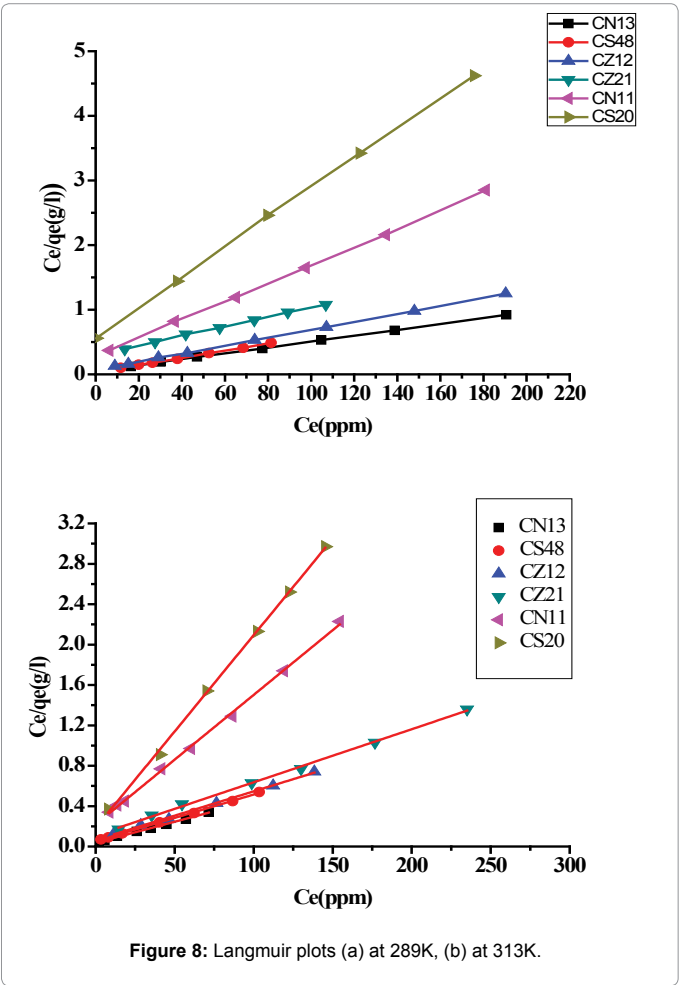
Figure 10: kinetics model for adsorption of methomyl (a) pseudo first order,(b) pseudo second order,(c) Intraparticule diffusion and (d) Boyd model.

The adsorption of methomyl onto the activated carbons reached equilibrium within about 60 min. The adsorption equilibrium could be well described by Langmuir adsorption isotherms, namely monolayer adsorption on a homogenous surface. The adsorption kinetics followed a pseudo-second order kinetic model and intra-particle diffusion was involved in the adsorption process. Thermodynamic results indicated that The Gibbs free energy change (ΔG°) was negative as expected for a spontaneous process under the applied conditions. The prepared ACPNS were successfully applied to the removal of methomyl from natural water samples.

References

1. Ninkovic MB, Petrovic RD, Lauševic MD (2010) Removal of organochlorine pesticides from water using virgin and regenerated granular activated carbon. J Serb Chem Soc 75: 565-573.

2. Chauhan RS, Singhal L (2006) Harmful effects of pesticides and their control through cowpathy. International Journal of Cow Science 2: 61-70.

3. Ritter L, Solomon K, Sibley P, Hall K, Keen P, et al. (2002) Sources, pathways, and relative risks of contaminants in surface water and groundwater: a perspective prepared for the Walkerton inquiry. J Toxicol Environ Health A 65: 1-142.

4. Dolan T, Howsam P, Parsons DJ, Whelan MJ (2013) Is the EU Drinking Water Directive Standard for Pesticides in Drinking Water Consistent with the Precautionary Principle? Environ sci technol 47: 4999-5006.

5. Van Scoy AR, Yue M, Deng X, Tjeerdema RS (2013) Environmental Fate and Toxicology of Methomyl, in Reviews of environmental contamination and toxicology. Springer 93-109.

6. El-Wakeil N, Shalaby S, Abdou G, Sallam A (2013) Pesticide-Residue Relationship and Its Adverse Effects on Occupational Workers.

7. Gupta RC, Milatovic D (2012) Toxicity of organophosphates and carbamates. Marrs TC (ed) Royal Society of Chemistry, Cambridge, UK 104-136.

8. Pereira JL, Gonçalves F (2007) Effects of food availability on the acute and chronic toxicity of the insecticide methomyl to Daphnia spp. Sci Total Environ 386: 9-20.

9. Guitart R (2012) Pesticide Residues in Birds and Mammals. Pesticides: Evaluation of Environmental Pollution 393.

10. Murthy HMR, Manonmani HK (2007) Aerobic degradation of technical hexachlorocyclohexane by a defined microbial consortium. Journal of hazardous materials 149: 18-25.

11. Kansal SK, Sushil Kumar, Hassan Ali, Ahmed Kapoor, Seema Bahnemann, et al. (2013) Preparation, Characterization and Photocatalytic Activity of Nanosized ZnO for the Degradation of Rhodamine B Dye and Simulated Dyebath Effluent. Science of Advanced Materials 5: 630-636.

12. Katsumata H, Kobayashi T, Kaneco S, Suzuki T, Ohta K (2011) Degradation of linuron by ultrasound combined with photo-Fenton treatment. Chemical Engineering Journal 166: 468-473.

13. Banasiak LJ, Van der Bruggen B, Schäfer AI (2011) Sorption of pesticide endosulfan by electrodialysis membranes. Chemical Engineering Journal 166: 233-239.

14. Maldonado MI, Malato S, Pérez-Estrada LA, Gernjak W, Oller I, et al. (2006) Partial degradation of five pesticides and an industrial pollutant by ozonation in a pilot-plant scale reactor. J Hazard Mater 138: 363-369.

15. Akl MA, El-Asmy AA, Yossef WM (2005) Separation via flotation, spectrophotometric speciation, and determination of vanadium(IV) in wastes of power stations. Anal Sci 21: 1325-1335.

16. Akl MA (2001) Spectrophotometric and AAS determinations of trace zinc(II) in natural waters and human blood after preconcentration with phenanthraquinone monophenylthiosemicarbazone. Anal Sci 17: 561-564.

17. Zhou T, Teik-Thye Lim, Sze-Sze Chin, Fan AG (2011) Treatment of organics in reverse osmosis concentrate from a municipal wastewater reclamation plant: Feasibility test of advanced oxidation processes with/without pretreatment. Chemical Engineering Journal 166: 932-939.

18. Bhatnagar A, Minocha A (2006) Conventional and non-conventional adsorbents for removal of pollutants from water-a review. Indian journal of chemical technology 13: 203-217.

19. Swami D, Buddhi D (2006) Removal of contaminants from industrial wastewater through various non-conventional technologies: a review. International journal of environment and pollution 27: 324-346.

20. Chen Y, Wang K, Lou L (2004) Photodegradation of dye pollutants on silica gel supported TiO< sub> 2 particles under visible light irradiation. Journal of Photochemistry and Photobiology A: Chemistry 163: 281-287.

21. Ghorai S, Pant KK (2005) Equilibrium, kinetics and breakthrough studies for adsorption of fluoride on activated alumina. Separation and Purification Technology 42: 265-271.

22. Wang S, Peng Y (2010) Natural zeolites as effective adsorbents in water and wastewater treatment. Chemical Engineering Journal 156: 11-24.

23. Dai Cm, Geissen SU, Zhang YL, Zhang YJ, Zhou XF (2011) Selective removal of diclofenac from contaminated water using molecularly imprinted polymer microspheres. Environmental Pollution 159: 1660-1666.

24. Celik E, Hosik Park, Hyeongyu Choi, Heechul Choi (2011) Carbon nanotube blended polyethersulfone membranes for fouling control in water treatment. Water research 45: 274-282.

25. Konig TN, Shulami S, Rytwo G (2012) Brine wastewater pretreatment using clay minerals and organoclays as flocculants. Applied Clay Science 67-68: 119-124.

26. Mahmoodi NM, Salehi R, Arami M (2011) Binary system dye removal from colored textile wastewater using activated carbon: Kinetic and isotherm studies. Desalination 272: 187-195.

27. Al-Othman Z, Ali R, Naushad M (2012) Hexavalent chromium removal from aqueous medium by activated carbon prepared from peanut shell: Adsorption kinetics, equilibrium and thermodynamic studies. Chemical Engineering Journal 184: 238-247.

28. Ioannidou O, Zabaniotou A (2007) Agricultural residues as precursors for activated carbon production-A review. Renewable and Sustainable Energy Reviews 11: 1966-2005.

29. Yakout S (2013) Surface modification and characterization of a RS activated carbon: density, yield, XRD, ash, and moisture content. Desalination and Water Treatment 1-9.

30. El-Hendawy ANA, Samra SE, Girgis BS (2001) Adsorption characteristics of activated carbons obtained from corncobs. Colloids and Surfaces A: Physicochemical and Engineering Aspects 180: 209-221.

31. Foo K, Hameed B (2012) Coconut husk derived activated carbon via microwave induced activation: effects of activation agents, preparation parameters and adsorption performance. Chemical Engineering Journal 184: 57-65.

32. Sarc-Ozdemir C, Onal Y (2013) Error Anlaysis Studies of Dye Adsorption onto Activated Carbon From Aqueous Solutions. Particulate Science and Technology.

33. Akl MA, Yousef AM, AbdElnasser S (2013) Removal of Iron and Manganese in Water Samples Using Activated Carbon Derived from Local Agro-Residues. Journal of Chemical Engineering & Process Technology 4: 4.

34. Khalili NR, Marta Campbell, Giselle Sandi, Janusz Golaś (2000) Production of micro-and mesoporous activated carbon from paper mill sludge: I. Effect of zinc chloride activation. Carbon 38: 1905-1915.

35. Abechi SE, Gimba CE, Uzairu A, Dallatu YA (2013) Preparation and Characterization of Activated Carbon from Palm Kernel Shell by Chemical Activation. Res J Chem Sci 3: 54-61.

36. Krishnan KA, Anirudhan TS (2003) Removal of cadmium (II) from aqueous solutions by steam-activated sulphurised carbon prepared from sugar-cane bagasse pith: Kinetics and equilibrium studies. Water SA 29: 147-156.

37. Newcombe G, Morrison J, Hepplewhite C, Knappe DRU (2002) Simultaneous adsorption of MIB and NOM onto activated carbon: II. Competitive effects. Carbon 40: 2147-2156.

38. Ahmedna M, Marshall W, Rao R (2000) Surface properties of granular activated carbons from agricultural by-products and their effects on raw sugar decolorization. Bioresource technology 71: 103-112.

39. Mahalakshmy R, Indraneel P, Viswanathan B (2009) Surface functionalities of nitric acid treated carbon: A density functional theory based vibrational analysis. Indian J Chem A 48: 352-356.

40. Dutta T, Agashe HB, Garg M, Balakrishnan P, Kabra M, et al. (2007) Poly (propyleneimine) dendrimer based nanocontainers for targeting of efavirenz to human monocytes/macrophages in vitro. J Drug Target 15: 89-98.

41. Pal K, Banthia AK, Majumdar DK (2007) Preparation and characterization of polyvinyl alcohol-gelatin hydrogel membranes for biomedical applications. AAPS PharmSciTech 8: 21.

42. Pereira MFR, Soares SF, Orfao JJM, Figueiredo JL (2003) Adsorption of dyes on activated carbons: influence of surface chemical groups. Carbon 41: 811-821.

43. Attia AA, Shouman MA, El-Nabarawy T (2005) Sorption of Pb^{2+} Ions on to Activated Carbons Prepared from Olive Stones. Carbon Science 6: 141-147.

44. Salman J, Njoku V, Hameed B (2011) Bentazon and carbofuran adsorption onto date seed activated carbon: kinetics and equilibrium. Chemical Engineering Journal 173: 361-368.

45. Aguedach A, Brosillon S, Morvan J, Lhadi el K (2008) Influence of ionic strength in the adsorption and during photocatalysis of reactive black 5 azo dye on TiO_2 coated on non-woven paper with SiO_2 as a binder. J Hazard Mater 150: 250-256.

46. Pan C, Yang W, Jia W, Weng J, Tian H (2009) Management of Chinese patients with type 2 diabetes, 1998-2006: the Diabcare-China surveys. Curr Med Res Opin 25: 39-45.

47. Lagergren S (1898) About the theory of so-called adsorption of soluble substances. Kungliga Svenska Vetenskapsakademiens Handlingar 24: 1-39.

48. Ho YS, McKay G (1998) Sorption of dye from aqueous solution by peat. Chemical Engineering Journal 70: 115-124.

49. Weber W, Morris J (1962) Advances in water pollution research. in Proceedings of the First International Conference on Water Pollution Research.

50. Sun Q, Yang L (2003) The adsorption of basic dyes from aqueous solution on modified peat-resin particle. Water Res 37: 1535-1544.

51. Hameed BH, El-Khaiary MI (2008) Kinetics and equilibrium studies of malachite green adsorption on rice straw-derived char. J Hazard Mater 153: 701-708.

52. Lamia KA, Sachdeva UM, DiTacchio L, Williams EC, Alvarez JG, et al. (2009) AMPK regulates the circadian clock by cryptochrome phosphorylation and degradation. Science 326: 437-440.

53. Schipper ML, Cheng Z, Lee SW, Bentolila LA, Iyer G, et al. (2007) microPET-based biodistribution of quantum dots in living mice. J Nucl Med 48: 1511-1518.

54. Tan EK, Zhao Y, Skipper L, Tan MG, Di Fonzo A, et al. (2007) The LRRK2 Gly2385Arg variant is associated with Parkinson's disease: genetic and functional evidence. Hum Genet 120: 857-863.

55. Kushwaha S, Soni H, Ageetha V, Padmaja P (2013) An Insight Into the Production, Characterization, and Mechanisms of Action of Low-Cost Adsorbents for Removal of Organics From Aqueous Solution. Critical Reviews in Environmental Science and Technology 43: 443-549.